

Incorporation of Neptunium(V) and Iodate into a Uranyl Phosphate: Implications for Mitigating the Release of ^{237}Np and ^{129}I in Repositories

SHIJUN WU,^{†,*} FANRONG CHEN,[†]
ANTONIO SIMONETTI,[‡] AND
THOMAS E. ALBRECHT-SCHMITT^{*,†}

Guangzhou Institute of Geochemistry, Chinese Academy of Sciences (GIGCAS), Guangzhou 510640, China, and Department of Civil Engineering and Geological Sciences and Department of Chemistry and Biochemistry, University of Notre Dame, Notre Dame, Indiana 46556

Received January 12, 2010. Revised manuscript received March 1, 2010. Accepted March 3, 2010.

The simultaneous incorporation of IO_3^- and NpO_2^+ into $\text{Ba}_3(\text{UO}_2)_2(\text{HPO}_4)_2(\text{PO}_4)_2$ (BaUP), which serves as a model for uranyl alteration phases, was investigated. LA-ICP-MS data demonstrate that the incorporation of both of these species is significantly enhanced when they are present together. The most probable explanation is that charge balance is obtained by the coupled substitutions of $\text{NpO}_2^+ \leftrightarrow \text{UO}_2^{2+}$ and $\text{IO}_3^- \leftrightarrow \text{HPO}_4^{2-}$. According to the LA-ICP-MS results, in the absence of iodate as much as 2.91 ± 0.14 to $3.44 \pm 0.25\%$ of the uranium in BaUP can be replaced by neptunium. When iodate is present in the reaction, the amount of uranium substitution by neptunium increases to $6.05 \pm 0.65\%$ to $7.93 \pm 0.83\%$. The net increase for neptunium is $116 \pm 0.30\%$ to $225 \pm 0.25\%$. Similarly, in the absence of NpO_2^+ , iodate incorporation into BaUP reaches an I/U level of 0.0021 ± 0.0004 to 0.0038 ± 0.0005 ; whereas in its presence there is an increase to as much as $100 \pm 0.11\%$ to 0.0042 ± 0.0008 .

Introduction

Deep geological repositories are being considered and even used as a method for the permanent disposal of high-level radioactive waste (HLW). However, these storage sites may serve as the source of hazardous radionuclides in the long term. Owing to their radiotoxicity and long half-lives, ^{237}Np ($t_{1/2} = 2.14 \times 10^6$ years) and ^{129}I ($t_{1/2} = 1.57 \times 10^7$ years) warrant special considerations and concerns for nuclear waste storage on a geologic time scale. There is as much as 0.5 kg of ^{237}Np and 0.2 kg of ^{129}I in each metric ton of used nuclear fuel (1). It has been estimated that more than 3000 kg of ^{237}Np and 5068 kg ^{129}I has been released into the environment because of nuclear weapons testing and nuclear fuel reprocessing (2, 3). There have been a series of previous investigations that focused on the source, distribution, and migration of ^{237}Np (4–10) and ^{129}I (3, 11–25) in the environment. The mechanisms of transport and retardation of

radionuclides derived from nuclear fission, as well as actinides that are also present in either used nuclear fuel or dispersed by nuclear detonations, have been summarized (26). Within these mechanisms, mineralization and precipitation are very important for some radionuclides (8, 27–30).

During the long-term storage of HLW, the waste form will corrode, and secondary uranyl phases, such as uranyl hydroxides, silicates, and phosphates are expected to form (31–34). Burns et al. predicted that transuranium elements present in the waste (e.g., neptunium and plutonium) could be incorporated into these alteration products, decreasing their mobility in the environment (35). Chen et al. analyzed many uranyl alteration phases, and proposed that selenium can incorporate into uranyl minerals via anion substitution (36). It has been recently reported that ^{237}Np can incorporate into several uranyl hydroxides and uranyl silicates in the form of NpO_2^+ , which is the dominate form of neptunium in the environment under oxidizing conditions (37–43). Our previous studies have also shown that iodine in the form of iodate can incorporate into a uranyl silicate and several uranyl phosphates (44, 45). The substitution of NpO_2^+ for UO_2^{2+} creates a charge imbalance that requires additional alterations elsewhere in the crystal structure (37–42). On the other hand, there is excess positive charge in the structure once SiO_4^{4-} or PO_4^{3-} is substituted by IO_3^- (44, 45). Considering that coupled substitution occurs naturally (46–49), charge-balance might be obtained if NpO_2^+ and IO_3^- simultaneously incorporate into the same structure.

In our previous study, we found that the synthetic uranyl phosphate, $\text{Ba}_3(\text{UO}_2)_2(\text{HPO}_4)_2(\text{PO}_4)_2$ (BaUP), can uptake significant amounts IO_3^- by substituting for HPO_4^{2-} : $\text{IO}_3^- \leftrightarrow \text{HPO}_4^{2-}$ (45). Because of the common character of uranyl polyhedra in BaUP and typical uranyl hydroxides/uranyl silicates (37–43), it is likely that NpO_2^+ will also incorporate into BaUP via $\text{NpO}_2^+ \leftrightarrow \text{UO}_2^{2+}$. However, this creates a charge imbalance. This disparity might be corrected for by incorporating an anion of lower charge than phosphate, such as iodate. Thus, we propose that coupled substitution of NpO_2^+ and IO_3^- into BaUP might occur to obtain charge balance. The goal of the work described herein was to determine how the presence of NpO_2^+ influences the uptake of IO_3^- and vice versa. In particular, we wanted to resolve whether the complementary charges of these ions would favorably influence their incorporation into a uranyl phosphate that serves as a model of a uranyl alteration phase.

Experimental Section

Syntheses. $^{237}\text{NpO}_2$ (99.9%, Oak Ridge), $\text{UO}_2(\text{NO}_3)_2 \cdot 6\text{H}_2\text{O}$ (98%, International Bio-Analytical Industries), H_3BO_3 (99.99%, Alfa-Aesar), H_3PO_4 (85%, Alfa-Aesar), BaCO_3 (99.8%, Alfa-Aesar), and HIO_3 (99.5%, Alfa-Aesar) were used as received. Distilled and Millipore filtered water with a resistance of 18.2 $\text{M}\Omega \cdot \text{cm}$ was used in all reactions. Reactions were run in Parr 4749 autoclaves with custom-made 10-mL polytetrafluoroethylene liners. **Caution:** ^{237}Np represents a serious health risk owing to its α and γ emission, and especially because of its decay to the short-lived isotope ^{233}Pa ($t_{1/2} = 27.0$ days), which is a potent β and γ emitter. All studies were conducted at the University of Notre Dame, which has appropriate equipment and personnel for handling such materials.

Incorporation of Neptunium and Iodate into BaUP. BaUP was synthesized using the method of Ling et al. (45). To study the incorporation of neptunium and iodate into BaUP, a solution of HIO_3 , NpO_2^+ , and $\text{HIO}_3/\text{NpO}_2^+$ was added into the starting solution of BaUP. The samples were labeled as BaUPI, BaUPNp, and BaUPINp, respectively. It is important

* Corresponding author e-mail: talbrec1@nd.edu; phone: (574) 631-1872; fax: (574) 631-9236.

[†] GIGCAS.

[‡] University of Notre Dame.

TABLE 1. Experimental Details for the Incorporation of NpO_2^+ and IO_3^- (mmol)

sample	UN ^a	BaCO ₃	H ₃ BO ₃	H ₃ PO ₄	H ₂ O	HIO ₃ ^b	NpO ₂ ⁺
BaUPI	0.345	1.035	0.345	1.035	6.944	3.451×10^{-2}	—
BaUPNp	0.345	1.035	0.345	1.035	27.778	—	1.875×10^{-2}
BaUPINp	0.345	1.035	0.345	1.035	—	3.451×10^{-2}	1.875×10^{-2}

^a UN = $\text{UO}_2(\text{NO}_3)_2 \cdot 6\text{H}_2\text{O}$. ^b HIO₃ solution was 0.069 mmol/L.

TABLE 2. Crystallographic Information of BaUP and Iodate/Neptunium Incorporated BaUP

sample	color	<i>a</i> (Å)	<i>b</i> (Å)	<i>c</i> (Å)	β (°)	<i>V</i> (Å ³)	crystal system	space group	reference
BaUP	yellow–green	9.51	8.70	10.54	97.31	865	mono.	<i>P</i> ₂ /c (No. 14)	Ling et al. 2009
BaUPI	yellow–green	9.52	8.68	10.54	97.23	865	mono.	<i>P</i> ₂ /c (No. 14)	this study
BaUPNp	green	9.51	8.69	10.55	97.20	864	mono.	<i>P</i> ₂ /c (No. 14)	this study
BaUPINp	green	9.52	8.70	10.54	97.34	866	mono.	<i>P</i> ₂ /c (No. 14)	this study

to note that BaUPNp and BaUPI are devoid of iodine and neptunium, respectively. The details of the experimental conditions used to study the incorporation of iodate and NpO_2^+ are listed in Table 1.

A NpO_2^+ stock solution was made as follows: NpO_2 was dissolved in 8 M HNO_3 at 200 °C in an autoclave. The resulting solution was reduced to a residue with heating, and then dissolved in water, yielding a pink solution containing exclusively NpO_2^{2+} . A large excess of NaNO_2 was added, reducing the Np(VI) to Np(V). $\text{NpO}_2(\text{OH})$ was precipitated by the addition of NH_4OH . The resulting solid was filtered off, washed, and dissolved in water with the minimal amount of HCl needed to achieve complete dissolution. The final concentration of Np(V) was 0.15 M. The products listed in Table 1 were washed with water and ethanol, and the crystals were left to dry in the air.

Crystallographic Studies. Single crystals of BaUPI, BaUPNp, and BaUPINp were selected and mounted on glass fibers with epoxy and aligned on a Bruker APEXII Quazar CCD X-ray diffractometer with a digital camera to determine unit cell parameters.

Laser-Ablation Inductively Coupled Plasma Mass Spectrometer (LA-ICP-MS) Analysis. Laser ablation analysis of single crystals from the three samples was conducted using a ThermoFinnigan high-resolution magnetic sector Element2 ICP-MS instrument coupled to a UP213 Nd:YAG laser ablation system (New Wave Research). Selected crystals were fixed on 1-in. glass slides with double-sided tape. Individual analyses consisted of 60 s measurement of background ion signals followed by a 60 s interval of measurement of ion signals subsequent to the start of lasering. Each analysis represents a total of 93 scans (93 runs \times 1 pass) with a sample (dwell) time of 0.01 s with 20 samples per ion signal peak. Analyses were conducted in medium mass resolution mode (resolution = mass/peak width \sim 4000) to eliminate possible spectral interferences, in particular between Np and U ion signals. The ablated particles were transported from the ablation cell to the ICP-MS instrument using He carrier gas at a flow rate of 0.7 L/min. Crystals were ablated using a range of spot sizes between 40 and 55 μm , repetition rate of 2 Hz, and 70% power output corresponding to an energy density of 12–15 J/cm². Using these ablation conditions, the depth of penetration of the laser is between \sim 5 and 15 μm (50, 51). Owing to the high content of ²³⁸U in the crystals, the ²³⁵U ion signal was measured to determine the ratios, and the total uranium content was calculated according to the abundance of ²³⁵U in depleted uranium, which was measured independently using solution ICP-MS. The depleted uranium used in this work contains 0.35% ²³⁵U. Based on the known

U content in BaUP, the iodine and Np concentrations were estimated on the basis of the ratios of the counts for I/U or Np/U.

Results and discussion

Syntheses. BaUP forms yellow–green crystals, and its structure was recently reported by us (45). The color does not change when iodine is incorporated into the structure. However, the neptunium-incorporated crystals are green. Buck et al. also found a similar color change when they studied the incorporation of neptunium into uranophane (43).

Crystallographic Studies. Crystallographic studies show that BaUPI, BaUPNp, and BaUPINp have the same unit cell parameters compared with BaUP (Table 2).

These data indicate that the average structure of BaUP is unaltered after iodine and neptunium incorporated into the matrix. Klingensmith et al. reported that the single crystal structure of metaschoepite also remains unchanged after neptunium incorporation (38). Our previous work also shows similar trends associated with trace iodate incorporation into several uranyl phosphates (45).

LA-ICP-MS. As shown in Figure 1, before the laser ablation begins background ion signals are both stable and very low. Once the laser shutter opened, stable peaks for ¹²⁷I and ²³⁷Np were observed, indicating that iodine and neptunium have been incorporated into the structure of BaUP. Furthermore, the neptunium signal is in accord with uranium as ablation continues from the surface of the crystal into the interior. The laser ablation cell was rastered during the lasering since crystals were ablated rapidly, especially the ones on the smaller end of the spectrum. This movement resulted in a bimodal distribution of ion signals (Figure 1), especially for BaUPI and BaUPNp. When performing the calculation, the signals from 60 s to 120 s were used to calculate the concentration and 1 s to 60 s were used as background. At least three separate crystals were analyzed for each sample.

According to the LA-ICP-MS results, the ratio of Np/U ranges from 0.0243 ± 0.0014 to 0.0356 ± 0.0025 in BaUPNp, which indicates that more than $2.91 \pm 0.14\%$ to $3.44 \pm 0.25\%$ of the uranium has been substituted by neptunium (Table 3). The uranium content in BaUP is 35.68%, and thus there is as much as $0.87 \pm 0.05\%$ to $1.27 \pm 0.09\%$ neptunium in BaUPNp. When iodate is present, the ratio of Np/U increased from 0.0644 ± 0.0065 to 0.0861 ± 0.0084 in BaUPINp, indicating $6.05 \pm 0.65\%$ to $7.93 \pm 0.83\%$ of the uranium has been substituted by neptunium, and the weight percent of neptunium is $2.16 \pm 0.23\%$ to $2.83 \pm 0.30\%$. The net increase rate for neptunium is $116 \pm 0.30\%$ to $225 \pm 0.25\%$. This is the highest neptunium content recorded within uranyl

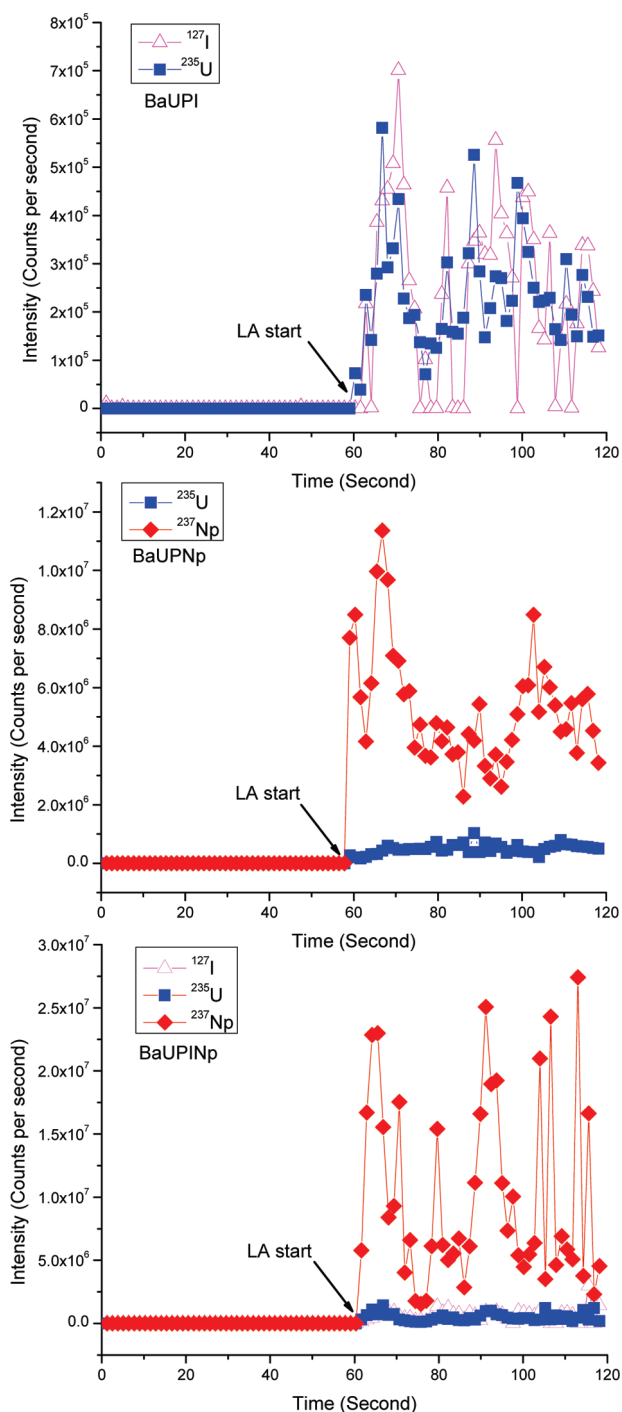


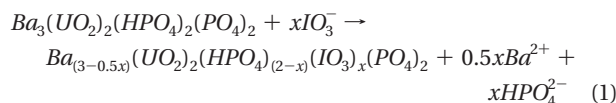
FIGURE 1. Typical LA-ICP-MS spectra for BaUPI, BaUPNp, and BaUPINp.

TABLE 3. Concentration of Neptunium and Iodine in BaUP

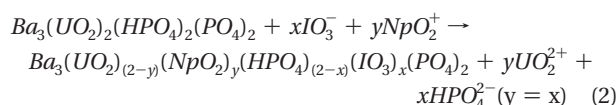
sample	molar ratio of I/U	molar ratio of Np/U	²³⁷ Np (wt %)	molar ratio of Np/I
BaUPINp	0.0042 ± 0.0008 ^a	0.0697 ± 0.0099	0.0231 ± 0.0035	15.3910 ± 0.0100
	0.0040 ± 0.0005 ^a	0.0861 ± 0.0084	0.0282 ± 0.0030	19.7499 ± 0.0084
	0.0041 ± 0.0006 ^a	0.0644 ± 0.0065	0.0221 ± 0.0023	14.7673 ± 0.0065
BaUPNp	—	0.0356 ± 0.0025	0.0122 ± 0.0009	—
	—	0.0243 ± 0.0014	0.0084 ± 0.0005	—
	—	0.0308 ± 0.0034	0.0106 ± 0.0012	—
BaUPI	0.0038 ± 0.0005	—	—	—
	0.0021 ± 0.0004	—	—	—
	0.0022 ± 0.0003	—	—	—

^a The molar ratio of I/U in BaUPINp was calculated as I/(Np+U).

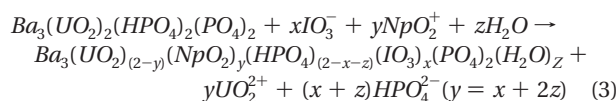
SCHEME 1.



SCHEME 2.



SCHEME 3.



compounds with incorporated neptunium content in metaschoepite being 500 ppm (38). On the other hand, the molar ratio of I/U in BaUPI ranges from 0.0021 ± 0.0004 to 0.0038 ± 0.0005, compared to 0.0040 ± 0.0005 to 0.0042 ± 0.0008 in BaUPINp with a 5.26 ± 0.84% to 100 ± 0.11% increase.

BaUP has two different PO₄³⁻ sites, P(1)O₄³⁻ and HP(2)O₄²⁻. It is unlikely that substitution of IO₃⁻ ↔ P(1)O₄³⁻ will happen because this would disrupt the structural connectivity. On the other hand, substitution of IO₃⁻ ↔ HP(2)O₄²⁻ is possible since only one UO₇ bipyramid is connected to HP(2)O₄²⁻ by corner-sharing. More details have been reported by Ling et al (45). As shown in Scheme 1, when IO₃⁻ is substituted for HPO₄²⁻, some Ba²⁺ should be lost between the layers to obtain charge-balance (45).

Np⁵⁺ usually exits as the neptunyl ion, NpO₂⁺, surrounded by 4–6 oxygen donors to yield tetragonal, pentagonal (dominate), or hexagonal bipyramids (52). The similarity of the geometries of the neptunyl (NpO₂⁺) and uranyl (UO₂²⁺) ions facilitates their substitution (35). Meanwhile, a charge-balancing substitution is also required elsewhere in the crystal structure when NpO₂⁺ substitutes for UO₂²⁺ (37–42). There is considerably more iodine and neptunium in BaUPINp compared to BaUPI and BaUPNp. The most probable explanation is that charge balance is obtained by the coupled substitutions of NpO₂⁺ ↔ UO₂²⁺ and IO₃⁻ ↔ HPO₄²⁻. If this is the correct mechanism, the ratio of Np/I in BaUPINp should be 1. Therefore, the mechanism should be described as in Scheme 2.

However, the ratio of Np/I in BaUPINp is as high as 14.7673 ± 0.0065 to 19.7499 ± 0.0084, demonstrating that more neptunium has been incorporated into the crystal. A possible mechanism for the higher neptunium concentration is that some of the HPO₄²⁻ has been substituted for H₂O, which can be expressed as Scheme 3.

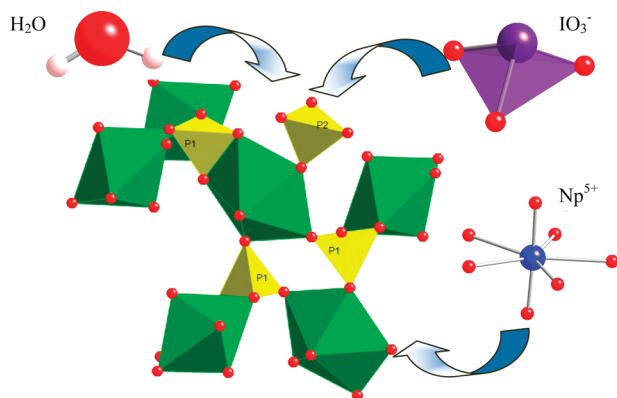


FIGURE 2. An illustration of the potential substitution of IO_3^- , NpO_2^+ , and H_2O in $\text{Ba}_3(\text{UO}_2)_2(\text{HPO}_4)_2(\text{PO}_4)_2$. Uranyl polyhedra are shown in green and phosphate polyhedra are shown in yellow. Oxygen atoms are shown in red.

We can speculate that these substitutions might occur as shown graphically in Figure 2.

Implications for the Retardation of the Release of Radionuclides in HLW Repositories. The molar ratios of $^{129}\text{I}/\text{U}$ and $^{237}\text{Np}/\text{U}$ in used nuclear fuel are about 4×10^{-4} and 5×10^{-4} , which are 1–2 orders of magnitude lower than that in BaUPINp. This indicates that the release of ^{129}I and ^{237}Np in repositories should be mitigated by incorporation into some alteration phases similar to BaUP. The radionuclides within the waste form, such as ^{137}Cs , ^{235}U , ^{237}Np , ^{239}Pu , ^{79}Se , ^{99}Tc , and ^{129}I , can be divided into cations and anions. In the previous studies, the retardation of cationic and anionic radionuclides was investigated separately even though they exist together in the waste form (37–45). Since coupled substitution of $\text{NpO}_2^+ \leftrightarrow \text{UO}_2^{2+}$ and $\text{IO}_3^- \leftrightarrow \text{HPO}_4^{2-}$ is observed in BaUP, a model for uranyl alteration phases, it provides an enhanced mechanism for mitigating the release of ^{129}I and ^{237}Np from a nuclear waste repository. Similar phenomena for coupled substitution are expected to occur in other uranyl phases, such as uranyl silicates and carbonates. Furthermore, coupled substitution of other cationic and anionic radionuclides is also expected.

Acknowledgments

We are grateful for support provided by the U.S. Department of Energy, Office of Civilian Radioactive Waste Management, Office of Science and Technology and International, through a subcontract with Argonne National Laboratory, and the National Natural Science Foundation of China (Grant 40972213). We are also thankful to anonymous reviewers for detailed and constructive comments that improved the quality and clarity of this manuscript.

Supporting Information Available

UV–vis–NIR spectra of all samples studied in this work were obtained from single crystals using a Craic Technologies microspectrophotometer. This material is available free of charge via the Internet at <http://pubs.acs.org>.

Literature Cited

- Mtingwa, S. K. Feasibility of Transmutation of Radioactive Elements. In *An International Spent Nuclear Fuel Storage Facility-Exploring a Russian Site as a Prototype: Proceedings of an International Workshop*; Schweitzer, G. E., Sharber, A. C., Eds.; The National Academies Press: Washington, DC, 2005; pp 30–49.
- Hemberger, P. H.; Efurud, D. W.; Rokop, D. J. Environmental Analysis of Transuranic Nuclides. In *Production and Measurement of Minor Actinides in the Commercial Fuel Cycle*; Stanbro, W. D., Ed.; Los Alamos National Laboratory: Los Alamos, NM, 1997.

- Aldahan, A.; Alifimov, V.; Possnert, G. ^{129}I anthropogenic budget: Major sources and sinks. *Appl. Geochem.* **2007**, *22* (3), 606–618.
- Müller, K.; Foerstendorf, H.; Brendler, V.; Bernhard, G. Sorption of Np(V) onto TiO_2 , SiO_2 , and ZnO : An in situ ATR FT-IR spectroscopic study. *Environ. Sci. Technol.* **2009**, *43* (20), 7665–7670.
- Wu, T.; Amayri, S.; Drebert, J.; Loon, L. R. V.; Reich, T. Neptunium(V) sorption and diffusion in opalinus clay. *Environ. Sci. Technol.* **2009**, *43* (17), 6567–6571.
- Efurud, D. W.; Runde, W.; Banar, J. C.; Janecy, D. R.; Kaszuba, J. P.; Palmer, P. D.; Roensch, F. R.; Tait, C. D. Neptunium and plutonium solubilities in a Yucca Mountain groundwater. *Environ. Sci. Technol.* **1998**, *32* (24), 3893–3900.
- Kaszuba, J. P.; Runde, W. H. The aqueous geochemistry of neptunium: Dynamic control of soluble concentrations with applications to nuclear waste disposal. *Environ. Sci. Technol.* **1999**, *33* (24), 4427–4433.
- Heberling, F.; Brendebach, B.; Lindqvist-Reis, P.; Bauer, A.; Bosbach, D. Neptunium(V) incorporation into calcite. *Geochim. Cosmochim. Acta* **2008**, *72* (12), A361–A361.
- Arai, Y.; Moran, P. B.; Honeyman, B. D.; Davis, J. A. In situ spectroscopic evidence for neptunium (V)-carbonate inner-sphere and outer-sphere ternary surface complexes on hematite surfaces. *Environ. Sci. Technol.* **2007**, *41* (11), 3940–3944.
- Icopini, G. A.; Boukhalfa, H.; Neu, M. P. Biological reduction of Np(V) and Np(V) citrate by metal-reducing bacteria. *Environ. Sci. Technol.* **2007**, *41* (8), 2764–2769.
- Schink, D. R.; Santschi, P. H.; Corapcioglu, O.; Sharma, P.; Fehn, U. ^{129}I in Gulf of Mexico waters. *Earth Planet. Sci. Lett.* **1995**, *135* (1–4), 131–138.
- Raisbeck, G. M.; You, F.; Zhou, Z. Q.; Kilius, L. R. ^{129}I from nuclear fuel reprocessing facilities at Sellafield (U.K.) and La Hague (France): Potential as an oceanographic tracer. *J. Marine Syst.* **1995**, *6* (5–6), 561–570.
- Chao, J.-H.; Tseng, C.-L. ^{129}I concentrations of mammalian thyroids in Taiwan. *Sci. Total Environ.* **1996**, *193* (2), 111–119.
- Wagner, M. J. M.; Dittrich-Hannen, B.; Synal, H. A.; Suter, M.; Schotterer, U. Increase of ^{129}I in the environment. *Nucl. Instrum. Meth. B* **1996**, *113* (1–4), 490–494.
- Rao, U.; Fehn, U. The distribution of ^{129}I around West Valley, an inactive nuclear fuel reprocessing facility in Western New York. *Nucl. Instrum. Meth. B* **1997**, *123* (1–4), 361–366.
- Edmonds, H. N.; Smith, J. N.; Livingston, H. D.; Kilius, L. R.; Edmond, J. M. ^{129}I in archived seawater samples. *Deep-Sea Res. Pt. I* **1998**, *45* (7), 1111–1125.
- Raisbeck, G. M.; You, F. ^{129}I in the oceans: Origins and applications. *Sci. Total Environ.* **1999**, *237–238*, 31–41.
- Hou, X. L.; Dahlgard, H.; Nielsen, S. P.; Ding, W. J. Iodine-129 in human thyroids and seaweed in China. *Sci. Total Environ.* **2000**, *246* (2–3), 285–291.
- Fehn, U.; Snyder, G. ^{129}I in the southern hemisphere: Global redistribution of an anthropogenic isotope. *Nucl. Instrum. Meth. B* **2000**, *172* (1–4), 366–371.
- Oktay, S. D.; Santschi, P. H.; Moran, J. E.; Sharma, P. ^{129}I and ^{127}I transport in the Mississippi River. *Environ. Sci. Technol.* **2001**, *35* (22), 4470–4476.
- Kekli, A.; Aldahan, A.; Meili, M.; Possnert, G.; Buraglio, N.; Stepanauskas, R. ^{129}I in Swedish rivers: Distribution and sources. *Sci. Total Environ.* **2003**, *309* (1–3), 161–172.
- Santos, F. J.; Lopez-Gutierrez, J. M.; Garcia-Leon, M.; Suter, M.; Synal, H. A. Determination of $^{129}\text{I}/^{127}\text{I}$ in aerosol samples in Seville (Spain). *J. Environ. Radioact.* **2005**, *84* (1), 103–109.
- Aldahan, A.; Kekli, A.; Possnert, G. Distribution and sources of ^{129}I in rivers of the Baltic region. *J. Environ. Radioact.* **2006**, *88* (1), 49–73.
- Persson, S.; Aldahan, A.; Possnert, G.; Alifimov, V.; Hou, X. ^{129}I Variability in precipitation over Europe. *Nucl. Instrum. Meth. B* **2007**, *259* (1), 508–512.
- Aldahan, A.; Persson, S.; Possnert, G.; Hou, X. L. Distribution of ^{129}I and ^{127}I in precipitation at high European latitudes. *Geophys. Res. Lett.* **2009**, *36* (11), L11805.
- Jedinakova-Krizova, V. Migration of radionuclides in the environment. *J. Radioanal. Nucl. Chem.* **1998**, *229* (1–2), 13–18.
- Nico, P. S.; Stewart, B. D.; Fendorf, S. Incorporation of oxidized uranium into Fe (Hydr)oxides during Fe(II) catalyzed remineralization. *Environ. Sci. Technol.* **2009**, *43* (19), 7391–7396.
- Kutty, K. V. G.; Asuvathraman, R.; Madhavan, R. R.; Jena, H. Actinide immobilization in crystalline matrix: A study of uranium incorporation in gadolinium zirconate. *J. Phys. Chem. Solids* **2005**, *66* (2–4), 596–601.

- (29) Stipp, S. L. S.; Christensen, J. T.; Lakshtanov, L. Z.; Baker, J. A.; Waight, T. E. Rare earth element (REE) incorporation in natural calcite: Upper limits for actinide uptake in a secondary phase. *Radiochim. Acta* **2006**, *94* (9–11), 523–528.
- (30) Kim, C.-W.; Wronkiewicz, D. J.; Finch, R. J.; Buck, E. C. Incorporation of cerium and neodymium in uranyl phases. *J. Nucl. Mater.* **2006**, *353* (3), 147–157.
- (31) Finch, R. J.; Ewing, R. C. The corrosion of uraninite under oxidizing conditions. *J. Nucl. Mater.* **1992**, *190*, 133–156.
- (32) Forsyth, R. S.; Werme, L. O. Spent fuel corrosion and dissolution. *J. Nucl. Mater.* **1992**, *190*, 3–19.
- (33) Wronkiewicz, D. J.; Bates, J. K.; Gerding, T. J.; Veleckis, E.; Tani, B. S. Uranium release and secondary phase formation during unsaturated testing of UO₂ at 90 °C. *J. Nucl. Mater.* **1992**, *190*, 107–127.
- (34) Wronkiewicz, D. J.; Bates, J. K.; Wolf, S. F.; Buck, E. C. Ten-year results from unsaturated drip tests with UO₂ at 90°C: Implications for the corrosion of spent nuclear fuel. *J. Nucl. Mater.* **1996**, *238* (1), 78–95.
- (35) Burns, P. C.; Ewing, R. C.; Miller, M. L. Incorporation mechanisms of actinide elements into the structures of U⁶⁺ phases formed during the oxidation of spent nuclear fuel. *J. Nucl. Mater.* **1997**, *245* (1), 1–9.
- (36) Chen, F.; Burns, P. C.; Ewing, R. C. ⁷⁹Se: Geochemical and crystallo-chemical retardation mechanisms. *J. Nucl. Mater.* **1999**, *275* (1), 81–94.
- (37) Klingensmith, A. L.; Burns, P. C. Neptunium substitution in synthetic uranophane and soddyite. *Am. Mineral.* **2007**, *92* (11–12), 1946–1951.
- (38) Klingensmith, A. L.; Deely, K. M.; Kinman, W. S.; Kelly, V.; Burns, P. C. Neptunium incorporation in sodium-substituted metaseboepite. *Am. Mineral.* **2007**, *92* (4), 662–669.
- (39) Douglas, M.; Clark, S. B.; Friese, J. I.; Arey, B. W.; Buck, E. C.; Hanson, B. D. Neptunium(V) partitioning to uranium(VI) oxide and peroxide solids. *Environ. Sci. Technol.* **2005**, *39* (11), 4117–4124.
- (40) Burns, P. C.; Deely, K. M.; Skanthakumar, S. Neptunium incorporation into uranyl compounds that form as alteration products of spent nuclear fuel: Implications for geologic repository performance. *Radiochim. Acta* **2004**, *92* (3), 151–159.
- (41) Burns, P. C.; Klingensmith, A. L. Uranium mineralogy and neptunium mobility. *Elements* **2006**, *2*, 351–356.
- (42) Buck, E. C.; Finch, R. J.; Finn, P. A.; Bates, J. K. Retention of neptunium in uranyl alteration phases formed during spent fuel corrosion. In *Scientific Basis for Nuclear Waste Management XXI*; Mc Kinley, I. G., McCombie, C. H., Eds.; Mater. Res. Soc. Symp. Proc., 1998; pp 87–94.
- (43) Buck, E. C.; Douglas, M.; McNamara, B. K.; Hanson, B. D. *Possible Incorporation of Neptunium in Uranyl (VI) Alteration Phases*; Pacific Northwest National Laboratory: Richland, WA, 2003.
- (44) Wu, S.; Chen, F.; Kang, M.; Yang, Y.; Dou, S. Incorporation of iodine into uranophane formed during the corrosion of spent nuclear fuel. *Radiochim. Acta* **2009**, *97* (8), 459–465.
- (45) Ling, J.; Wu, S.; Chen, F.; Simonetti, A.; Shafer, J. T.; Albrecht-Schmitt, T. E. Does iodate incorporate into layered uranyl phosphates under hydrothermal conditions? *Inorg. Chem.* **2009**, *48* (23), 10995–11001.
- (46) Binder, G.; Troll, G. Coupled anion substitution in natural carbon-bearing apatites. *Contrib. Mineral. Petr.* **1989**, *101* (4), 394–401.
- (47) Carpena, J.; Boyer, L.; Fialin, M.; Kienast, J. R.; Lacout, J. L. Ca²⁺, PO₄³⁻ ↔ Ln³⁺, SiO₄⁴⁻ coupled substitution in the apatitic structure: Stability of the mono-silicated fluor-britholite. *C. R. Acad. Sci. Paris* **2001**, *333* (7), 373–379.
- (48) Fleet, M. E.; Liu, X. Coupled substitution of type A and B carbonate in sodium-bearing apatite. *Biomaterials* **2007**, *28* (6), 916–926.
- (49) Pan, Y.; Fleet, M. Compositions of the Apatite-Group Minerals: Substitution Mechanisms and Controlling Factors. In *Phosphates: Geochemical, Geobiological, and Materials Importance*; Kohn, M. J., Rakovan, J., Hughes, J. M., Eds.; Mineralogical Society of America: Washington, DC, 2002; pp 13–50.
- (50) Simonetti, A.; Heaman, L. M.; Chacko, T.; Banerjee, N. R. In-situ petrographic thin section U-Pb dating of zircon, monazite, and titanite using laser ablation-MC-ICP-MS. *Int. J. Mass Spectrom.* **2006**, *253*, 87–97.
- (51) Simonetti, A.; Heaman, L. M.; Chacko, T. Use of discrete-dynode secondary electron multipliers with Faradays - A 'reduced volume' approach for in-situ U-Pb dating of accessory minerals within petrographic thin section by LA-MC-ICP-MS. In *2008 V.M. Goldschmidt Laser Ablation Short Course 40*; Sylvester, P., Ed.; Vancouver, BC, 2008; pp 241–264.
- (52) Forbes, T. Z.; Wallace, C.; Burns, P. C. Neptunyl compounds: Polyhedron geometries, bond-valance parameters, and structural hierarchy. *Can. Mineral.* **2008**, *46*, 1623–1645.

ES100115K